ORIGINAL ARTICLE

Index of Metallic Taste from Lightness Distribution of Real Images

Takumi ISHIWATA ＊, Kishio TAMURA ＊ and Akihiko ITAMI ＊

Abstract

As one of the high-value-added prints, embellished metallic prints via digital on-demand metallic foil printing have been of interest. Due to their eye-catching appearance, they are suitable for commercial prints, such as cosmetic packages and advertisements. Despite an expanding market, color management of the metallic prints still depends on visual judgment and the prescribed index of metallic taste has not yet been defined. Since the absence of an index has decreased productivity of people involved in this market, such an index based on perception has been needed. Thus, we suggest an index calculated from the lightness distribution of the real metallic images. The index possessed a linear correlation with perception and distinguished several appearances of the metallic images. It should be useful for several creative scenes in this market.

Keywords

Printing, Metallic appearance, Psychophysical metrics

1 Introduction

Psychophysical metrics about the relationship between vision, perception and appearance have significantly contributed to industry. As the representative example, the $L^*a^*b^*$ colorimetric system has successfully provided a methodology to quantify the color of prints. It is regarded as one of the uniform color spaces and regarding the uniform and linear correlation with perceived magnitude, it is useful and widely utilized in industry such as the quality control of product color. Thus, the correlation between perception and appearance of common colors, such as red and yellow, have been studied for long time.

On the other hand, the correlation between the perception and appearance of metallic colors, such as gold and silver, is unexpectedly still under study and has been of interest in recent decades [1-8]. For instance, Okajima et al. reported the importance of luminance distribution for metallic recognition [1]. In addition to this, several factors for metallic recognition have been reported such as the specular/diffuse ratio [2, 3], lighting condition [4, 5], surface irregularity [6], shape recognition [7], observation area [8], etc. Although these research studies certainly indicate that the recognition of metallic colors is different from common colors, the prescribed method and index for quantification of metallic image based on perception is not defined, presumably due to the difficulties from said multidimensional recognition factors.

It is a serious issue for players who engage in embellished metallic prints such as designers, printing operators and foil makers. Due to the absence of an appropriate index for quantifying the metallic appearance, many inefficiencies have been caused. That is, designers cannot explain details of their design of metallic prints by a quantitative representation, thus the printing operators cannot choose a suitable foil species for requirement from the designers, etc. The

＊ Corporate R&D Headquarter, Advanced Technology Center, Konica Minolta, Inc., 2970 Ishikawa-machi, Hachioji-shi, Tokyo 192-8505, Japan

color management of foils has also depended on the visual judgement due to the lack of an index and the dependence has decreased productivity of this market. These inefficiencies have caused time loss and cost and interfered with market expansion. This fact strongly prompted us to study which physical features of metallic prints induce the metallic taste and then construct the index. We now suggest a metallic taste index (MTI) possessing a linear correlation with the perceived magnitude.

To construct the index, we focused on the lightness distribution of the reflection as a feature of the unique metallic appearance. Fig. 1 a)-b) shows a comparison of the lightness distribution property between the common colors and metallic colors. Regarding the common colors, almost all the incident light is reflected as diffuse light and the distribution becomes nearly isotropic. On the other hand, the lightness distribution of metallic colors is quite anisotropic, and the incident light is predominantly reflected around specular. This is significantly characteristic for metallic images, and a recent study demonstrated that specular, roughness and diffusion of the metallic lightness distribution stimulate a specific brain area [9, 10]. Thus, it should be considered for the construction of the index. A diagram of our strategy is shown in Fig. 1 c). In this research, the lightness distributions were measured by goniometric spectrocolorimetry [11]. Subsequently, the distribution property was fitted by a Lorentzian curve (Eq. 1) so that the character of the distribution was mathematically explained. Eq. 2 then provided the MTI. The antilogarithm indicates the average lightness concentrated within the width of the half maximum of the specular distribution. The index becomes high if the distribution is sharp and strong, conversely, the index becomes low if the peak possesses a wide skirt.

$$f_n(\theta) = B + \sum_{i=1}^{n} g_i(\theta), \; g_i(\theta) = \frac{H_i w_i^2}{w_i^2 + (\theta - \theta_0)^2} \quad (1)$$

$$\mathrm{MTI} = \log\left[\frac{\int_{\theta_0 - w_n}^{\theta_0 + w_n} f_n(\theta)\, \mathrm{d}\theta}{2 w_n}\right] \quad (2)$$

n: Terms of fitting function (= 1 or 2),
B: Baseline,
θ_0:   Peak location,
H: Peak height,
w: Half width of half maximum.

Furthermore, we demonstrated the threshold between the terms of gloss-metallic, matte-metallic and non-metallic by using the MTI. In the metallic printing market, players often use terms such as Tsuya-Koutaku (gloss-metallic) and Keshi-Koutaku (matte-metallic), but these terms are not clearly defined. Our result of the threshold determination should provide definitions for the terms and contribute to the efficiency improvement of the color management of metallic images.

2 Experimental section

2.1 Materials

2.1.1 Metallic images for magnitude estimation

Ten kinds of metallic images (Image 1-10) were prepared for the magnitude estimation (Table 1).

2.1.2 Metallic images for threshold determination

The mirror-like aluminum deposited film (Image 18) and six kinds of diffusion films were prepared (Table 2).

Covering the aluminum deposited film with the diffusion films provided images with several appearances
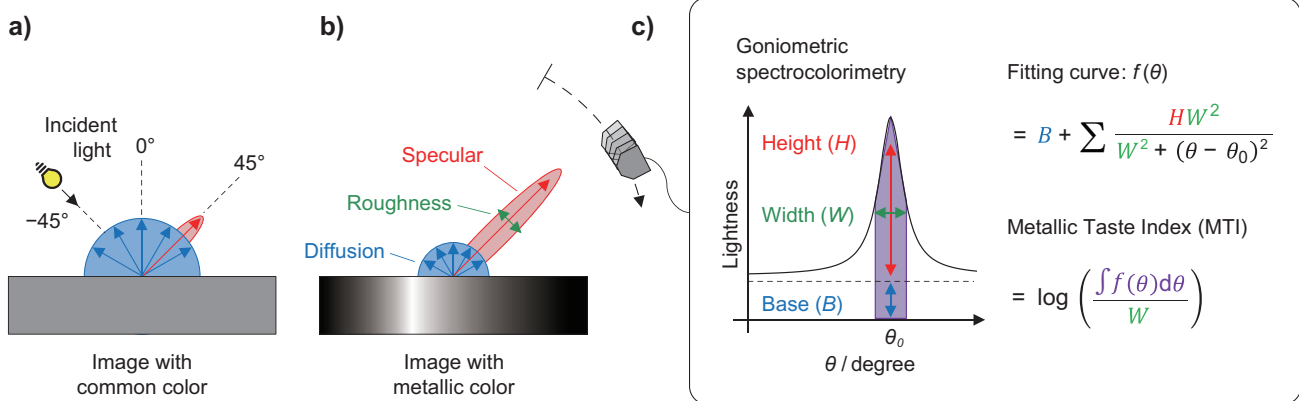

Fig. 1 Diagrams of lightness distribution of a) common colors and b) metallic colors. c) Concept of quantification for metallic images by lightness distribution.

(Images 11-16). Additionally, a standard silver foil image (Image 17) was added. Gold metallic images with several appearances were also prepared to obtain the threshold of the gold (Images 19-26).

Table 1 Appearance of Images 1-10.

No.	Appearance
Image 1	Gray image with slight gloss
Image 2	Gray image with slight gloss and irregularity
Image 3	Blight gray image
Image 4	Mirror-like image with haze
Image 5	Dark mirror-like image
Image 6	Folding-screen-like image
Image 7	Mirror-like image with slight haze
Image 8	Mirror-like image with slight hairline
Image 9	Mirror-like image with orange peel finish
Image 10	Mirror-like image

Table 2 Components of Images 11-26.

No.	Base	Haze of diffusion film
Image 11	Aluminum deposit film	92
Image 12	Aluminum deposit film	87
Image 13	Aluminum deposit film	82
Image 14	Aluminum deposit film	67
Image 15	Aluminum deposit film	46
Image 16	Aluminum deposit film	29
Image 17	Standard gloss silver foil	—
Image 18	Aluminum deposit film	—
Image 19	Gold deposit film	92
Image 20	Gold deposit film	87
Image 21	Gold deposit film	82
Image 22	Gold deposit film	67
Image 23	Gold deposit film	46
Image 24	Gold deposit film	29
Image 25	Standard gloss gold foil	—
Image 26	Gold deposit film	—

2. 2 Measurement

2. 2. 1 Goniometric spectrocolorimetry measurement

Preparation of the samples for the goniometric spectrocolorimetry measurement (Samples 1-26) are shown in **Fig. 2 a)-b)**. These samples possess a 15×50 mm metallic area on a 50×50 mm cardboard base. The measurement was carried out by goniometric spectrocolorimetry (Murakami Color Research Laboratory

Co., Ltd., GCMS-4) on the metallic area. The lightness distribution from 0 to 50 degrees was obtained at an incident light fixed at -45 degrees. The measurement intervals were 2 degrees and 1 degree for the measurement range from 0 to 30 degrees and from 30 to 50 degrees, respectively. D_{50} was selected as the light source condition.

2. 2. 2 Calculation of MTI

The obtained lightness distributions were fitted by a Lorentzian curve (Eq. 1, $n=1$) so that the distribution could be mathematically expressed. The fitting curve was estimated by a least square calculation using Excel solver. To briefly confirm the fitting accuracy, the correlation coefficient (R^2_{fit}) between the experiment and fitting values was calculated in the range from 0 to 45 degrees. For the R^2_{fit} of less than 0.98 and the skirt of the peak was underrated, fitting with two Lorentzian curves ($n=2$) was carried out for a precise fitting. Subsequently, Eq. 2 provided the MTI value.

2. 2. 3 Comparative index

For comparison of the suggested MTI, we calculated the Flop index (Eq. 3) [12], Contrast gloss (Eq. 4) [13], and Specular lightness (Eq. 5) as a comparative index. These L^* values were measured by the goniometric spectrocolorimetry in the same way.

$$\text{Flop Index} = \frac{2.69\,(L^*_{30}-L^*_{-65})^{1.11}}{L^{*\,0.86}_0} \quad (3)$$

$$\text{Contrast Gloss} = \frac{L^*_{45}}{L^*_0} \quad (4)$$

$$\text{Specular Lightness} = L^*_{45} \quad (5)$$

L^*: Lightness.
Subscripts show the number of receiver angles.

2. 3 Psychophysical experiments

2. 3. 1 Stimuli

Images 1-26 were masked by a white mask with a 15×15 mm square cutout. Attaching the masked images on circular cylindrical vials provided stimuli for the psychophysical experiment (Stimuli 1-26, **Fig. 2 c)**). Additionally, Stimuli 1'-26' were prepared using a black mask instead of the white masks (**Fig. 2 d)**). Stimuli 1-10 and Stimuli 11-26 were for the magnitude estimation and threshold determination, respectively.
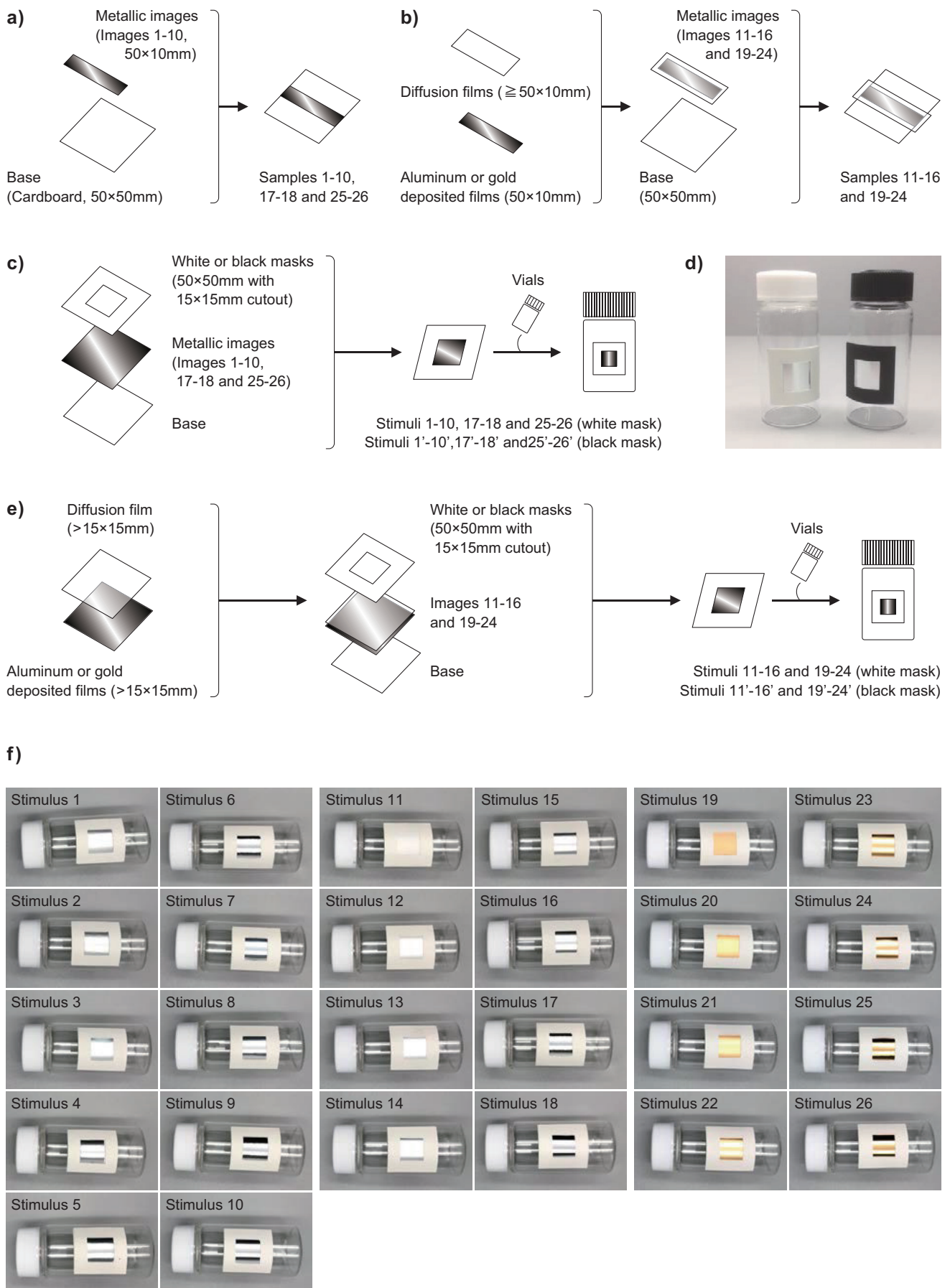
Fig. 2 Schematic diagrams of preparation of a) Samples 1-10, 17-18, 25-26, b) Samples 11-16, 19-24. c) Stimuli 1-10, 17-18, 25-26, 1'-10', 17'-18' and 25'-26'. d) Photograph of stimulus with white and black mask. e) Schematic diagram of preparation of Stimuli 11-16, 19-24, 11'-16' and 19'-24'. f) Photographs of Stimuli 1-26.

2.3.2 Observers

Twelve naive observers were assigned. The observers consisted of two males and two females from three generations, i.e., their twenties, thirties and forties.

2.3.3 Magnitude estimation

The observers could freely handle Stimuli 1-10 in the light booth (X-Right, Inc., Judge II) placed in a darkroom and observe the metallic images under the D_{50} standard light source. After their observations, they estimated the strength of the metallic taste from zero- (no metallic taste) to ten- (strong metallic taste) points. As references, gray paper and a mirror-like aluminum deposited film were presented as zero- and ten-point references, respectively. After observation of Stimuli 1-10, they repeated the same protocol using the black masked stimuli (Stimuli 1'-10'). The obtained scores were averaged and plotted with the values of the calculated indexes. The correlativity was evaluated by the correlation coefficiency (R^2_{index}) of the plot.

2.3.4 Threshold determination

The observers could freely handle Stimuli 11-18 in the light booth (X-Right, Inc., Judge QC) placed in a darkroom and observe the metallic images under the D_{50} standard light source. After their observations, the observers labeled the stimuli by three terms, non-metallic, matte-metallic and gloss-metallic. The perception probability curve of the gloss-metallic and matte-metallic were then separately calculated by fitting a sigmoid curve as shown by Eq. 6. The thresholds were determined from a middle point location.

$$\zeta(x) = \frac{1}{1 + \exp\ a(x_0 - x)} \tag{6}$$

a : Steepness,
x_0: Middle point location.

3 Results and discussion

3.1 Measurement of lightness distribution

As shown in Fig. 3 and Fig. 4, goniometric spectro-colorimetry of Images 1-10 afforded the lightness distribution. The shapes of the curves were well fitted by a Lorentzian distribution. Concerning Image 3, fitting with two Lorentzian curves was needed due to the poor fit of the peak skirt area (Fig. 4). Fig. 6 shows lightness distribution of Images 11-26. The reflection property of all the images was then mathematically explained.
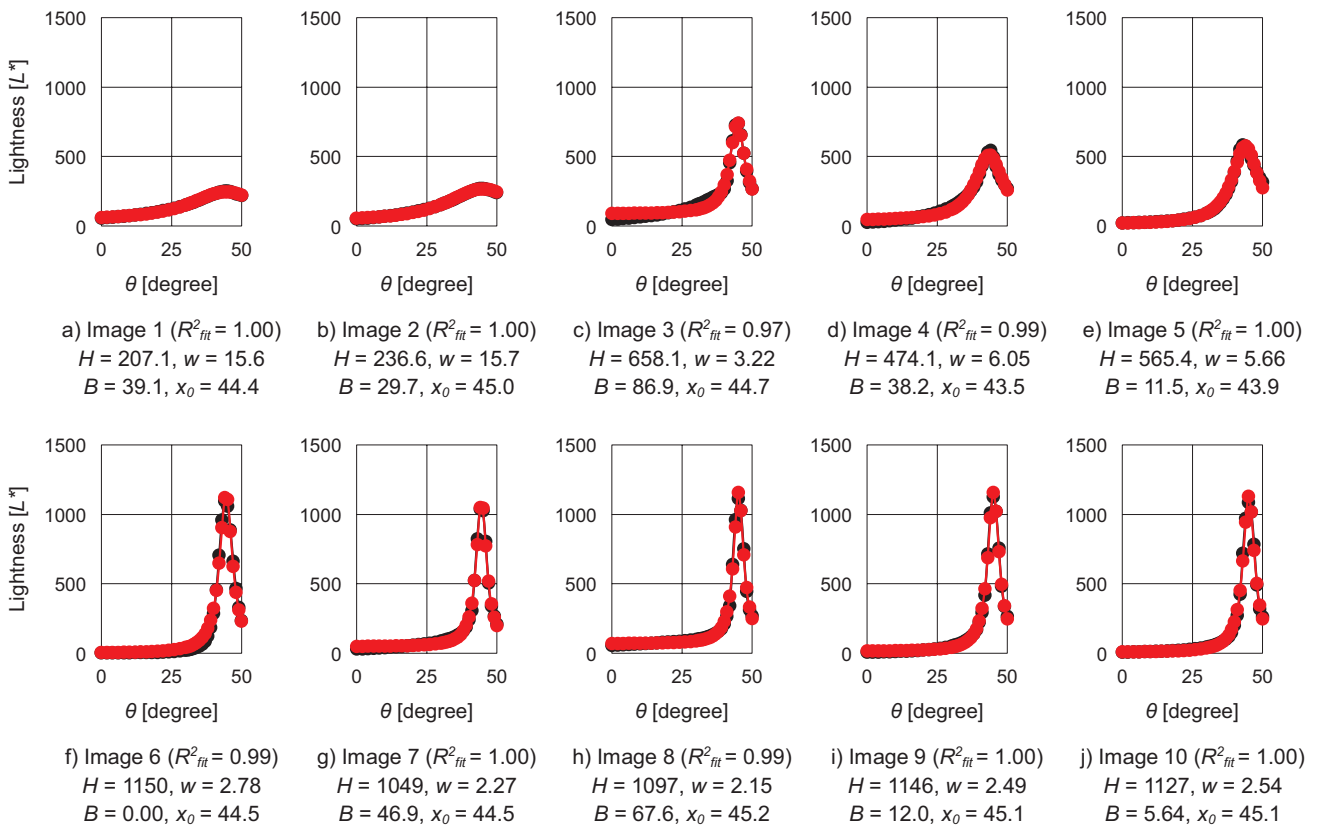

a) Image 1 (R^2_{fit} = 1.00)
H = 207.1, w = 15.6
B = 39.1, x_0 = 44.4

b) Image 2 (R^2_{fit} = 1.00)
H = 236.6, w = 15.7
B = 29.7, x_0 = 45.0

c) Image 3 (R^2_{fit} = 0.97)
H = 658.1, w = 3.22
B = 86.9, x_0 = 44.7

d) Image 4 (R^2_{fit} = 0.99)
H = 474.1, w = 6.05
B = 38.2, x_0 = 43.5

e) Image 5 (R^2_{fit} = 1.00)
H = 565.4, w = 5.66
B = 11.5, x_0 = 43.9

f) Image 6 (R^2_{fit} = 0.99)
H = 1150, w = 2.78
B = 0.00, x_0 = 44.5

g) Image 7 (R^2_{fit} = 1.00)
H = 1049, w = 2.27
B = 46.9, x_0 = 44.5

h) Image 8 (R^2_{fit} = 0.99)
H = 1097, w = 2.15
B = 67.6, x_0 = 45.2

i) Image 9 (R^2_{fit} = 1.00)
H = 1146, w = 2.49
B = 12.0, x_0 = 45.1

j) Image 10 (R^2_{fit} = 1.00)
H = 1127, w = 2.54
B = 5.64, x_0 = 45.1

Fig. 3 Lightness distributions of Images 1-10. Black and red lines indicate measured curve and fitted curve (n = 1), respectively.
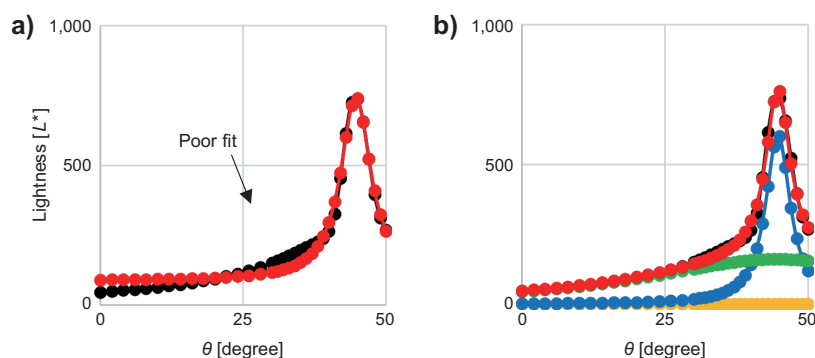
Fig. 4 a) Result of one peak fitting (n=1) of lightness distribution of Image 3. Black and red lines indicate measured curve and fitted curve (same with Fig. 3 c)), respectively. b) Result of two-peak fitting (n=2) of lightness distribution of Image 3. Black, red, blue, green and yellow lines indicate measured curve, fitted curve, first curve, second curve and baseline, respectively. The fitted curve was a combination of the first curve, second curve and baseline and the R^2_{fit} was 1.00.

3.2 Magnitude estimation

The obtained perceived magnitude (ϕ) and calculated values of the indexes are shown in **Table 3**. From the perceived magnitude, the prepared images seem to be sorted into three categories as low metallic taste (Images 1 and 2, ϕ=0-3), middle metallic taste (Images 3-5, ϕ=3-7) and high metallic taste (Images 6-10, ϕ=7-10). Regarding Images 6-10, the surface finishes, such as orange peel and hairline, were not significantly affected more than expected and all the ϕ values were greater than seven.

Concerning the Flop index and Contrast gloss, a slight correlation was observed in the low metallic taste domain. However, as shown in **Fig. 5 a)-b)**, no obvious correlation could be observed in the high metallic taste domain, and the R^2_{index} were 0.19 and 0.16 (**Table 3**). The Flop index is mainly utilized for evaluation of the metal flake pigment such as the paint of vehicles. Thus, this index presumably could not be adapted to the high metallic taste image. Alternatively, the Contrast gloss is calculated by dividing $L_{45}{}^*$ by $L_0{}^*$ and the value tend to be sensitive to $L_0{}^*$. Since $L_0{}^*$ of the high metallic taste images was a variable and independent of the metallic taste, the value was not correlated with the perceived magnitude and is presumably not suitable for evaluation of real metallic images.

For comparing the two indexes, the specular lightness showed a better correction. However, a mismatch was observed in the middle metallic area (**Fig. 5 c)**). In spite of the fact that the metallic taste of Image 3 was obviously lower than those of Images 4 and 5, the specular lightness value of Image 3 was higher than those of Images 4 and 5. The result indicated that the specular lightness overrated the gloss of Image 3 and the metallic taste could not be explained only by the specular intensity. The reasons should be the unique lightness distribution of Image 3. The peak possessed a strong and sharp main peak but also a weak and wide skirt at the bottom of the main peak. This indicated that the gloss contained a secondary component and the secondary broad reflection decreased the metallic taste of Image 3, regardless of the first sharp peak.

In that regard, the MTI could reflect the broadness of the secondary specular by a two-peak fitting process and as shown in **Fig. 5 d)**, the order between Images 3, 4 and 5 could be identical to the perceived magnitude. Therefore, it possessed a good correlation with the perception from the low to high metallic taste range and high R^2_{index}. This result indicated that the suggested MTI linearly correlated with human perception and provided a suitable index for quantifying the metallic taste of the images.

Table 3 Value of indexes and perceived magnitude.

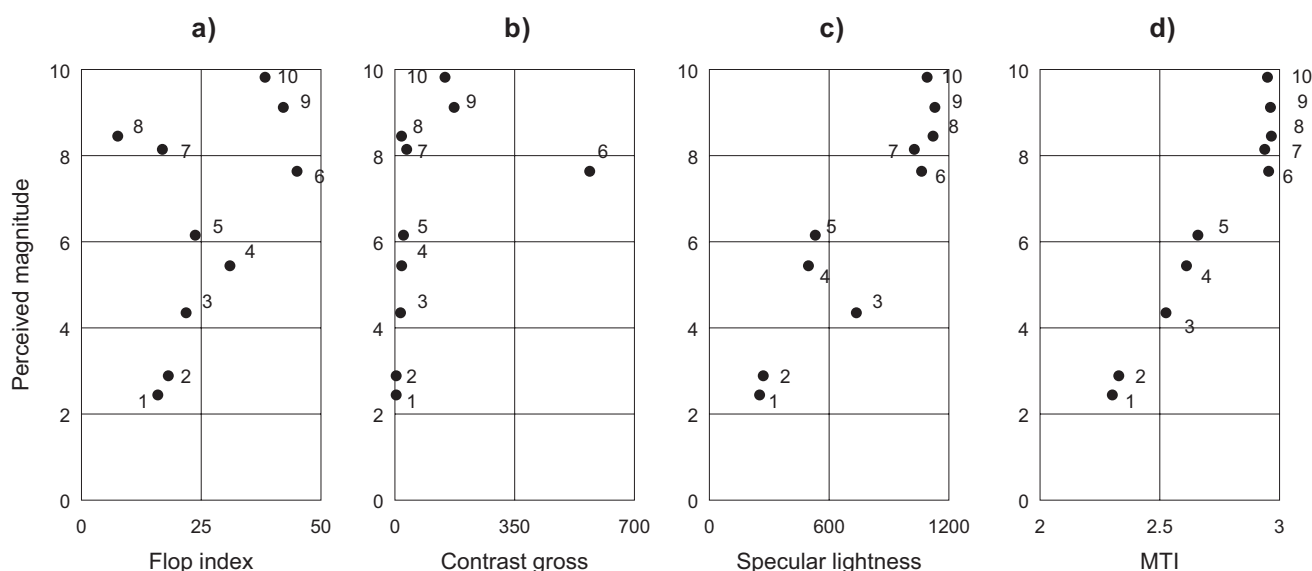| No.	φ	Flop index	Contrast gloss	Specular lightness	MTI
1	2.44	16.0	4.41	252.4	2.30
2	2.88	18.2	5.29	271.2	2.33
3	4.33	21.9	15.9	738.1	2.53
4	5.43	31.1	19.1	496.7	2.61
5	6.14	23.8	24.2	528.6	2.66
6	7.63	45.0	567	1059	2.96
7	8.12	17.0	34.6	1026	2.94
8	8.44	7.61	19.7	1115	2.97
9	9.10	42.3	173	1126	2.96
10	9.81	38.4	146	1085	2.95
R^2_{index}	—	0.19	0.16	0.86	0.95

Fig. 5 Correlativity evaluation between perceived magnitude and a) Flop index, b) Contrast gloss, c) Specular lightness and d) MTI. The numbers on each plot show the image number.

Furthermore, we confirmed the robustness of the MTI for individual variance. Table 4 shows individual R^2_{index} of the Flop index, Contrast gross, Specular lightness and MTI. Individual R^2_{index} of the MTI were higher than other indexes in every observer. This result suggested the MTI possess high robustness for individual variance.

Table 4 Individual R^2_{index}.

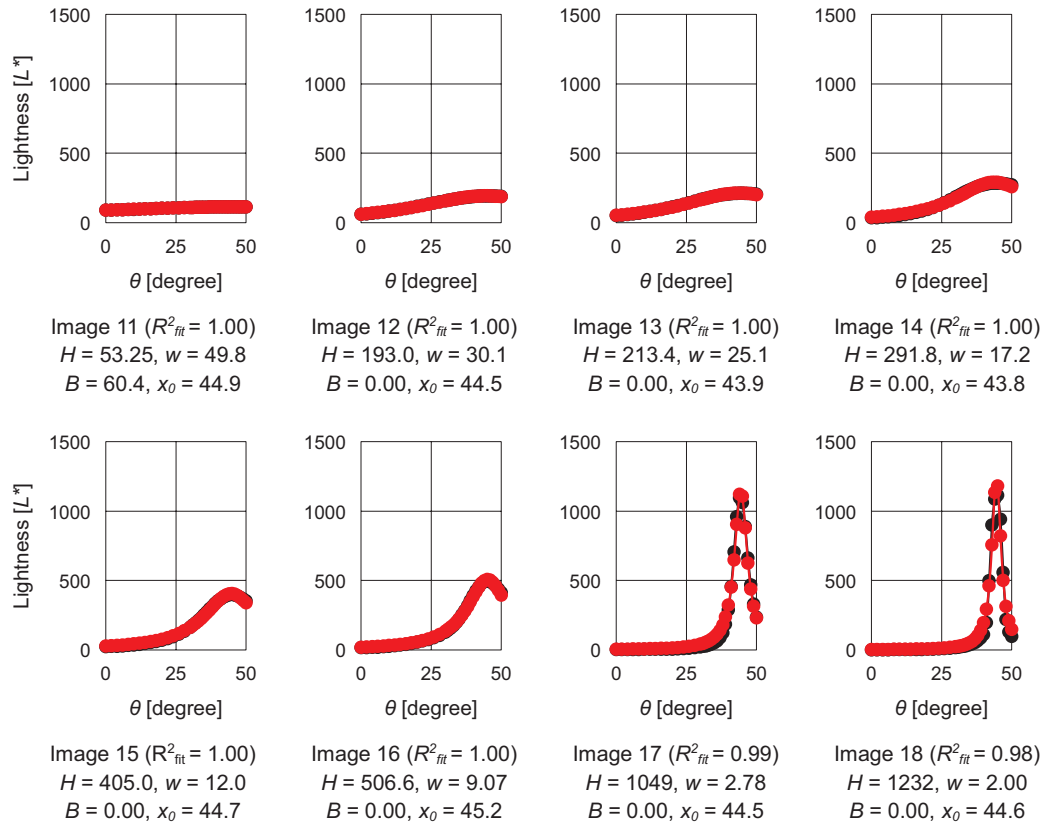| Observers	Flop index	Contrast gloss	Specular lightness	MTI
Observer A	0.11	0.13	0.84	0.95
Observer B	0.16	0.17	0.88	0.93
Observer C	0.18	0.12	0.87	0.88
Observer D	0.20	0.19	0.89	0.94
Observer E	0.13	0.07	0.82	0.87
Observer F	0.22	0.24	0.78	0.94
Observer G	0.12	0.09	0.75	0.89
Observer H	0.30	0.24	0.82	0.91
Observer I	0.34	0.27	0.81	0.90
Observer J	0.22	0.14	0.83	0.91
Observer K	0.15	0.13	0.85	0.95
Observer L	0.11	0.11	0.76	0.88

3. 3 Threshold determination

We further estimated the perceived thresholds between the gloss-metallic, matte-metallic and non-metallic appearances by using the MTI. The MTI values were calculated from lightness distributions of Images 11-26 shown in Fig. 6. The perception probability curve of the gloss-silver is shown as a red line

in Fig. 7 a). The half-value of the sigmoid curve indicated that the threshold between the gloss-silver and matte-silver was 2.74. Similarly, the blue line in Fig. 7 a) shows the perception probability between the matte-silver and non-silver and the threshold was 2.19. Furthermore, the threshold between the gloss-gold, matte-gold and non-gold were estimated to be 2.14 and 2.61, respectively (Fig. 7 b)). These results provided a numerical definition to the metallic foil terms such as Tsuya-Gin (gloss-silver), Keshi-Gin (matte-silver), Tsuya-Kin (gloss-gold) and Keshi-Kin (matte-gold). Concerning difference between threshold of Gloss-silver and Gloss-gold, threshold of Gloss-silver was higher than threshold of Gloss-gold. In this regard, Okajima et al. reported that recognition of Gloss-silver needed more reflectance than Gloss-gold [1]. Our result also indicated similar tendency.

Moreover, we constructed a color space for the metallic images by using the MTI, a^* and b^* values to demonstrate its application for color management. Fig. 8 shows the color space. Several terms were used for the appearances of popular gold foils such as Ao-Kin (Cold-gloss-gold) and Aka-Kin (Warm-glossgold). Hence, these colors should be numerically defined for color management. The MTI calculation and spectrophotometric analysis of the standard five foils, including Ao-Kin and Aka-Kin, then provided us the color space. It indicated that the combined use of the MTI, a^* and b^* could describe the precise appearance of the metallic foils. Additionally, combining the threshold could enhance the convenience of the color space. The result indicated that the MTI should contribute to color management of metallic images.

Silver (Image 11-18)

Image 11 (R^2_{fit} = 1.00)
H = 53.25, w = 49.8
B = 60.4, x_0 = 44.9

Image 12 (R^2_{fit} = 1.00)
H = 193.0, w = 30.1
B = 0.00, x_0 = 44.5

Image 13 (R^2_{fit} = 1.00)
H = 213.4, w = 25.1
B = 0.00, x_0 = 43.9

Image 14 (R^2_{fit} = 1.00)
H = 291.8, w = 17.2
B = 0.00, x_0 = 43.8

Image 15 (R$^2_{fit}$ = 1.00)
H = 405.0, w = 12.0
B = 0.00, x_0 = 44.7

Image 16 (R^2_{fit} = 1.00)
H = 506.6, w = 9.07
B = 0.00, x_0 = 45.2

Image 17 (R^2_{fit} = 0.99)
H = 1049, w = 2.78
B = 0.00, x_0 = 44.5

Image 18 (R^2_{fit} = 0.98)
H = 1232, w = 2.00
B = 0.00, x_0 = 44.6

Gold (Image 19-26)

Image 19 (R^2_{fit} = 1.00)
H = 54.18, w = 45.7
B = 55.1, x_0 = 47.2

Image 20 (R^2_{fit} = 1.00)
H = 180.4, w = 28.5
B = 0.00, x_0 = 45.7

Image 21 (R^2_{fit} = 1.00)
H = 199.3, w = 23.9
B = 0.00, x_0 = 44.0

Image 22 (R^2_{fit} = 1.00)
H = 272.2, w = 16.3
B = 0.00, x_0 = 43.8

Image 23 (R^2_{fit} = 1.00)
H = 373.1, w = 11.5
B = 0.00, x_0 = 44.9

Image 24 (R^2_{fit} = 1.00)
H = 456.5, w = 9.03
B = 0.00, x_0 = 44.3

Image 25 (R^2_{fit} = 0.98)
H = 981.5, w = 3.25
B = 0.00, x_0 = 45.6

Image 26 (R^2_{fit} = 0.99)
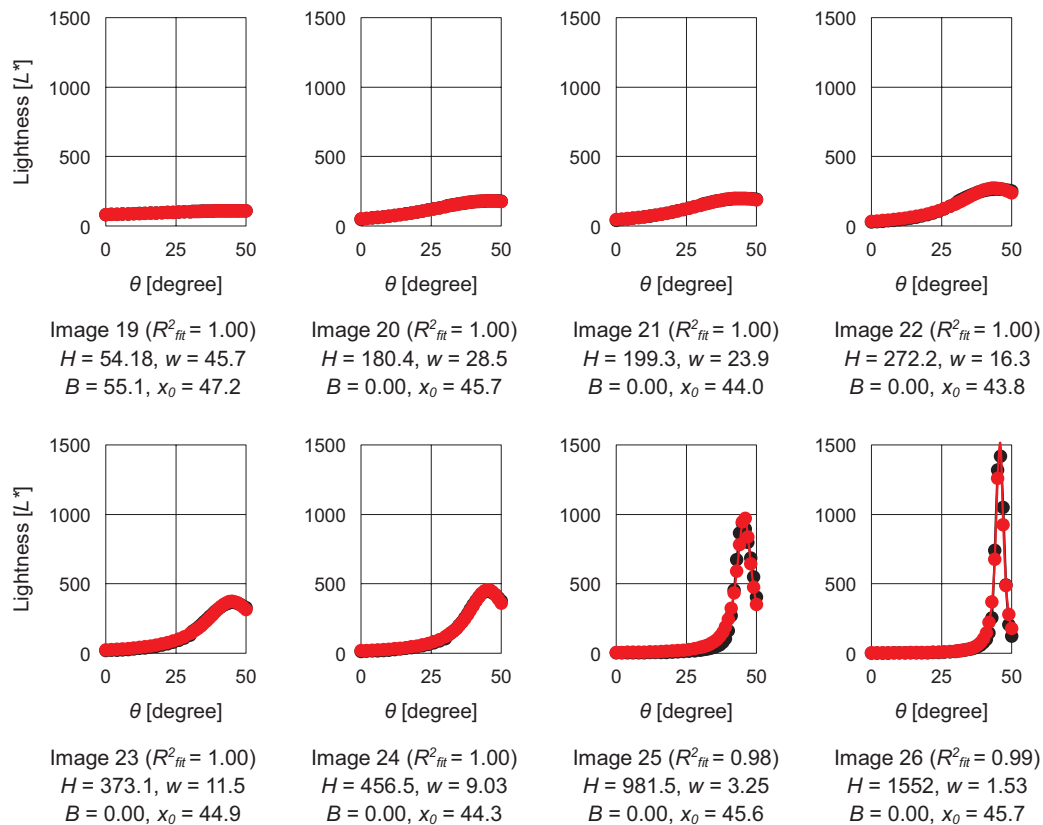H = 1552, w = 1.53
B = 0.00, x_0 = 45.7

Fig. 6 Lightness distributions of Images 11-26. Black and red lines indicate measured curve and fitted curve (n = 1), respectively.
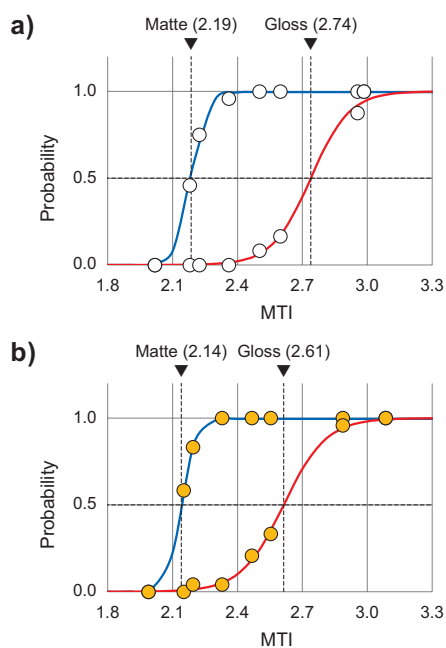
Fig. 7 Perception probability curves of a) silver and b) gold. Blue line indicates the threshold between non-metallic and matte-metallic taste. Red line indicates the threshold between matte-metallic and gloss-metallic appearances.
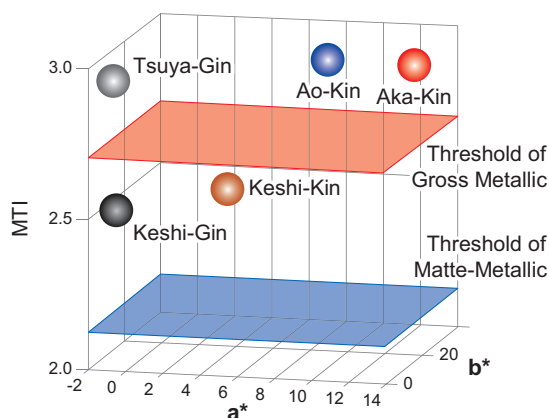

Fig. 8 Color space for quantification of metallic images using MTI as z-axis. a^* and b^* were obtained from specular component include (SCI) measurement of spectrophotometers (KONICA MINOLTA, INC., CM2600d). Red, blue, yellow, dark gray and gray spheres indicate standard Tsuya-Kin (Aka-Kin and Ao-Kin), Keshi-Kin, Tsuya-Gin and Keshi-Gin foils. Red plane indicates average threshold of gloss-silver and gloss-gold. Blue plane indicates average threshold of matte-silver and matte-gold.

4 Conclusion

In summary, we constructed an index of metallic taste from the lightness distribution of metallic images. It is suggested that the MTI possesses a linear correlation with the perception of metallic taste. Furthermore, the procedure could quantify the metallic taste of images with the unique lightness distribution property such as Image 3. The result indicated that the methodology is versatile for several real metallic images. Although the metallic appearance

tends to be already explained by using the specular and diffuse variables, the result also indicated that the appearance of real metallic images could not be quantified by only these two parameters and the shape of the lightness distribution, especially, the peak skirt should be considered for metallic quantification.

Moreover, the threshold between the gloss-metallic, matte-metallic and non-metallic could be clarified by using the MTI. Additionally, the three-dimensional color space consisting the MTI, a^* and b^* could visualize the precise appearance of metallic foils. This result would provide definition to the terms and be helpful for color management. To the best of our knowledge, a suitable index explaining the strength of the metallic taste of embellished metallic prints does not exist and the absence has restricted the growth of the metallic print market. We hope our results would contribute to support business expansion of the printing market.

References
1. Okajima, K., Nasu, S., and Takase, M.; Image condition and recognition mechanism for metallic color perception, Journal of the Color Science Association of Japan, 22 (Suppl.), pp. 14–15, 1998. (in Japanese)
2. Okazawa, G., Koida, K., and Komatsu, H.; Categorical properties of the color term "GOLD", Journal of Vision, 11(8), pp. 1–19, 2011.
3. Matsumoto, T., Fukuda, K., and Uchikawa, K.; Appearance of gold, silver and copper colors of glossy object surface, International Journal of Affective Engineering, 15(3), pp. 239–247, 2016.
4. Daira, T., and Omodani, M.; Clarification of gold color recognition mechanism – A study on the effects of lighting condition –, Journal of the Imaging Society of Japan, 50(6), pp. 498–502, 2011. (in Japanese)
5. Olkkonen, M., and Brainard, D. H.; Perceived glossiness and lightness under real-world illumination, Journal of Vision, 10(9), pp. 1–19, 2010.
6. Miyatani, Y., and Omodani, M.; Recognition mechanism of the gold/silver color – Evaluation of recognition transition from mirror appearance to silver/gold –, Journal of the Imaging Society of Japan, 54(2), pp. 115–122, 2015. (in Japanese)
7. Kojima, S., and Omodani, M.; Recognition mechanism for gold color – Confirmation of necessity of shape recognition as a requirement for gold color recognition –, Journal of the Imaging Society of Japan, 46(5), pp. 357–362, 2007. (in Japanese)
8. Koizumi, Y., Omodani, M., and Takahashi, Y.; Clarifying the mechanism for perceiving gold and silver color by studying recognition behavior within limited observation area, Journal of the Imaging Society of Japan, 40(3), pp. 209–213, 2001. (in Japanese)
9. Nishio, A., Goda, N., and Komatsu, H.; Neural selectivity and representation of gloss in the monkey inferior temporal cortex, The Journal of Neuroscience, 32(31), pp. 10780–10793, 2012.

10. Nishio, A., Shimokawa, T., Goda, N., and Komatsu, H.; Perceptual gloss parameters are encoded by population responses in the monkey inferior temporal cortex, 34(33), pp. 11143–11151, 2014.

11. Mori, E.; Guide for goniometric spectrocolorimetry, Journal of the Imaging Society of Japan, 44(6), pp. 476–488, 2005. (in Japanese)

12. McCamy, C. S.; Observation and measurement of the appearance of metallic materials: Part I. Macro appearance, Color Research and Application, 21(4), pp.292-304, 1996.

13. Hunter, S.; Methods of determining gloss, Journal of Research of the National Bureau of Standard, 18, pp. 19–39, 1937.

Takumi ISHIWATA (Non-member)

Takumi Ishiwata Ph. D. is an assistant manager of Konica Minolta Inc. He received bachelor's degree, master's degree and Ph. D. in chemistry from Hokkaido university, Japan, in 2011, 2013 and 2016, respectively. In 2012, He was engaged in research of crystal engineering at the Strasbourg university, France. In 2013, He was engaged in research of organic synthesis at the University of California, Sun Diego, USA. From 2013 to 2016, He was JSPS research fellow DC1 and engaged in research of polymer science and supramolecular chemistry. Since 2016, he joined Konica Minolta Inc. He is engaged in new business development relating imaging, psychophysics, electromagnetics, informatics, etc. He received various awards including the 35th Inoue research award for young scientists.

Kishio TAMURA (Non-member)

Kishio Tamura is a R&D team manager of special ink products for an inkjet presses in Konica Minolta Inc. He received B. Eng. and M. Eng. of chemical engineering from Nagoya university, Japan, in 1988 and 1990 respectively. He had been involved in R&D of chemical products for electronic photo copiers and printers in Konica corp. since 1990. After Konica corporation and Minolta corporation were merged and Konica Minolta Inc. was founded in 2003, he had expanded his R&D field to smart chemicals for agriculture and holographic materials for smart glasses in the company. Another his field is robust quality engineering. He received paper awards of Robust Quality Engineering Society (RQES) in 2000 and 2004. He has been in charge of the chairperson of the award committee in RQES since 2018.

Akihiko ITAMI (Non-member)

Akihiko Itami received his B.S. and M.S. degrees in organic chemistry from Tsukuba University, Japan, in 1985 and 1987, respectively. He joined Konishiroku Shashin Kogyo Inc. (now Konica Minolta Inc.) in 1987 and was engaged in R&D of the organic photoreceptors, the dye-sensitized solar cells, the functional inks and Kansei imaging. He was a senior manager of the advanced imaging R&D division of Konica Minolta Inc. and a director of the Imaging Society of Japan.